Supporting Online Material for

Structural basis of silencing: Sir3 BAH domain in complex with a nucleosome at 3.0 Å resolution

Karim-Jean Armache, Joseph D. Garlick, Daniele Canzio, Geeta J. Narlikar, and Robert E. Kingston

§The correspondence should be addressed to REK (kingston@molbio.mgh.harvard.edu).

This PDF file includes

Materials and Methods

Complex preparation and crystallization

The S.*cerevisiae* Sir3p BAH D205N was a generous gift of Dr. R. Sternglanz (*55*). The domain was expressed in BL21(DE3)pLysS E. coli as an C-terminal hexahistidine fusion at 18°C. The BAH domain was purified by metal affinity chromatography using NiNTA resin (Qiagen), and further purified to homogeneity on HiPrep Q 16/10 FF anion exchange column and Superdex 200 26/60 size exclusion chromatography (GE Healthcare). Recombinant *Xenopus* core histones were expressed, purified and assembled with a variant of the Widom 601 DNA sequence with three altered residues (see PDB) into the nuclesome core particle essentially as described (*56*). The complex of the BAH domain and nucleosome core particle was assembled by mixing the BAH domain with nucleosome core particle in a 3:1 molar ratio followed by Superose 6 size exclusion chromatography (GE Healthcare). The resultant complex was concentrated to 8-12 mg/ml and crystals were grown by vapor diffusion at 20°C using 4% PEG 400, 0.1 M potassium chloride, 0.01 M magnesium chloride and 0.05 M Hepes pH 7.0. Crystals were transferred from 0 to 27% PEG 400 in 2% increments with 10-15 minutes between each step. Crystals were then transferred to 4°C and after 12 hours flash frozen in liquid nitrogen for data collection. This post-crystallization cryo-treatment improved diffraction from 6Å to 3Å.

Data collection and crystallographic analysis

Diffraction data were collected using an ADSC Quantum 315 CCD detector at Advanced Photon Source's NE-CAT beamline 24-ID-E and the data processed using the iMosflm (*57*) and CCP4 package (*58*). The structure was solved by molecular replacement using Phaser (*59*) and a search model containing two rigid bodies: the histone octamer with histone tails removed , and the 147 bp human α-satellite DNA (PDB ID 1KX5 (*60*)) with the DNA bases manually changed to match the DNA sequence. The difference electron density map after one round of refinement of the molecular replacement solution showed clear positive electron density for the BAH on both sides of the nucleosome. This density was fitted with the BAH domain (1-214) (PDB ID 2FVU (*55*)) and crystallographic refinement was carried out using BusterTNT (*61*) and PHENIX (*62*) together with manual model building in COOT (*63*). The stereochemistry of the protein components was analyzed using Molprobity (*64*) and PROCHECK (*65*). Root mean square differences (rmsd) were calculated using the CCP4 package (*58*). All molecular graphics were prepared using PyMOL software (http://www.pymol.org/) with electrostatic potentials calculated using APBS (*66*). Secondary structure was analyzed using KSDSSP (*67*) and secondary structure figure prepared with help of JALVIEW (*68*).

Sedimentation Velocity Analytical Ultracentrifugation Studies

Sedimentation Velocity experiments were conducted using an analytical ultracentrifuge (Beckman Coulter) equipped with an absorption optical scanner. BAH protein was dialyzed overnight into 20mM Hepes 7.5, 150 mM NaCl, 1 mM DTT. The protein was then quantified by UV absorption at 280 nm. Serial dilutions were prepared to a final volume of 400μl and then placed in AUC chamber pre-equilibrated at 20°C and kept at zero-rpm at 20°C for 1 hour under vacuum. Runs were performed at 20°C at rotor speed of 50K rpm overnight. Scans were collected at 280-250-230 nm, with radial step size of 0.003 cm and continuous scanning mode at approximately one minute intervals. Data analysis was performed with the software SEDFIT, using a sedimentation coefficient distribution model *c(s)*. Peaks were integrated to determine the weighted-average sedimentation coefficients, and the data were assembled into an isotherm and analyzed with the software SEDPHAT with a dimerization model following the law of mass action. Protein partial specific volume, buffer density and buffer viscosity were obtained using the software SEDNTERP.

SOM Text

Additional information to complex preparation

Complexes formed between the WT Sir3 BAH domain and a nucleosome core particle were not stable as judged by size exclusion chromatography, whereas complexes of the nucleosome with BAHSir3 (which contains residues 1-214 of Sir3 D205N) co-migrated as a single peak following size exclusion chromatography. From this purified complex three-dimensional crystals were obtained which diffracted anisotropically to 4-6 Å. Post-crystallisation stabilization treatment reduced anisotropy and allowed collection of complete diffraction data to 3 Å.

Additional description of contacts in the H4 N-terminal tail: BAH domain interface. The majority of the interactions in this interface are shown in Fig. 3 and discussed in the main text and figure legends. Most electrostatic contacts between H4 and the BAH domain in this interface are mediated through side-chain interactions. Two of the important residues in BAH_{Sir3} identified in genetic screens, K209 and S212, form contacts with the H4 tail, with a potential hydrogen bond between K209 and the main chain carbonyl of H4 L22 and a van der Waals contact between S212 and H4 R23.

Additional description of contacts in the H4 and H2B cores: BAH interface.

The majority of the interactions in this interface are shown in Fig. 4a, c, d and discussed in the main text and figure legends. Two residues at the tip of the BAH_{Sir3} loop 3 (L79 and N80) interact extensively with both histone H4 and histone H2B. They make van der Waals contacts with histone H4 residues E74, H75 and K77. Additionally the BAH N80 side-chain could potentially form hydrogen bonds with main chain carbonyls of H4E74 and H2B R89. BAH residues N77, T78 and L79 can also interact with H2B residues in helices α3 and αC. Residue BAH K202 could potentially form a hydrogen bond with histone H4 residue E63. In a manner similar to reciprocal mutations in BAH D205 and H3D77, the LRS mutations can be suppressed by a gain-of-function mutation BAH L79I, also identified in the *slr* screen.

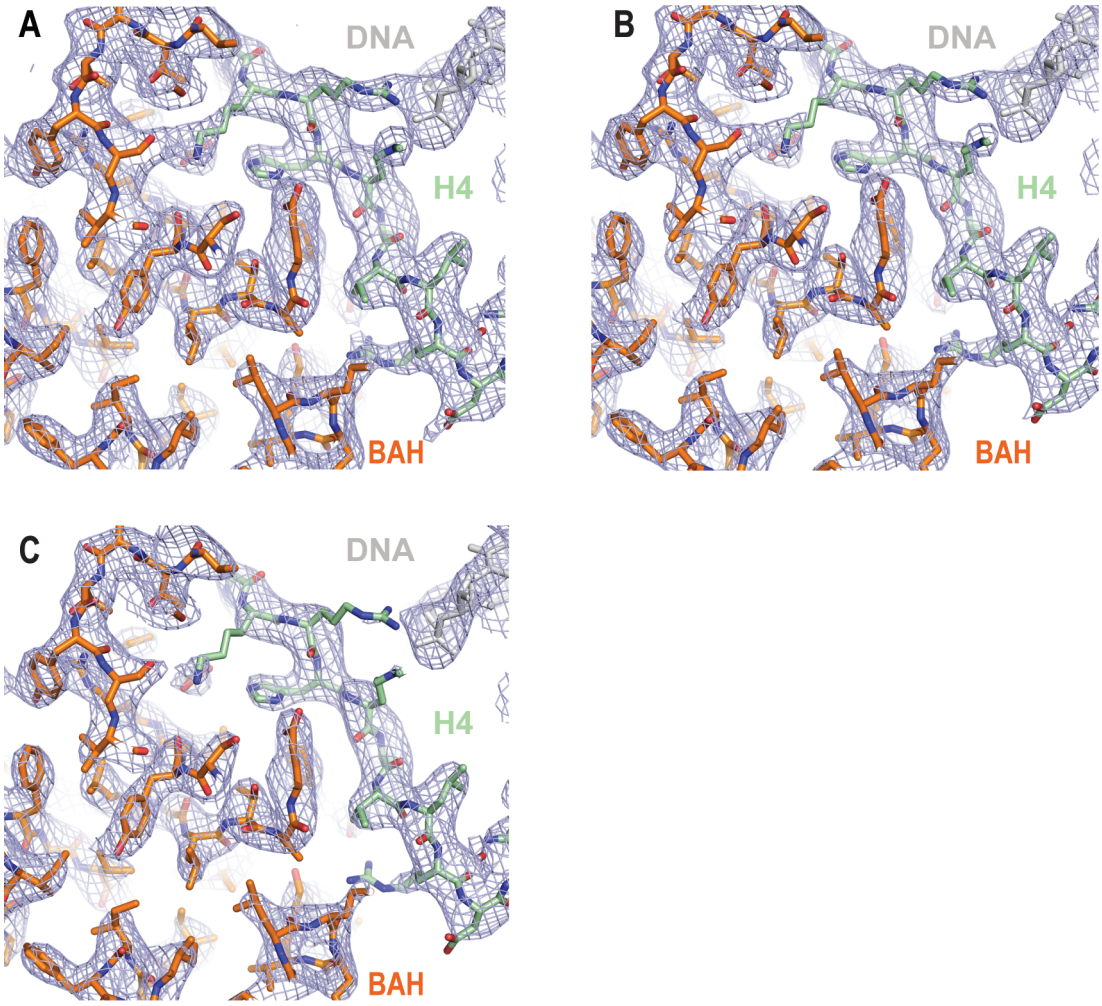

Fig. S1 Electron density maps
Maximum-likelihood $2mF_o$-DF_c difference Fourier electron density map for BAH-histone H4 interface contoured at 0.8 σ (**A**), 1.0 σ (**B**) and 1.5 σ (**C**)

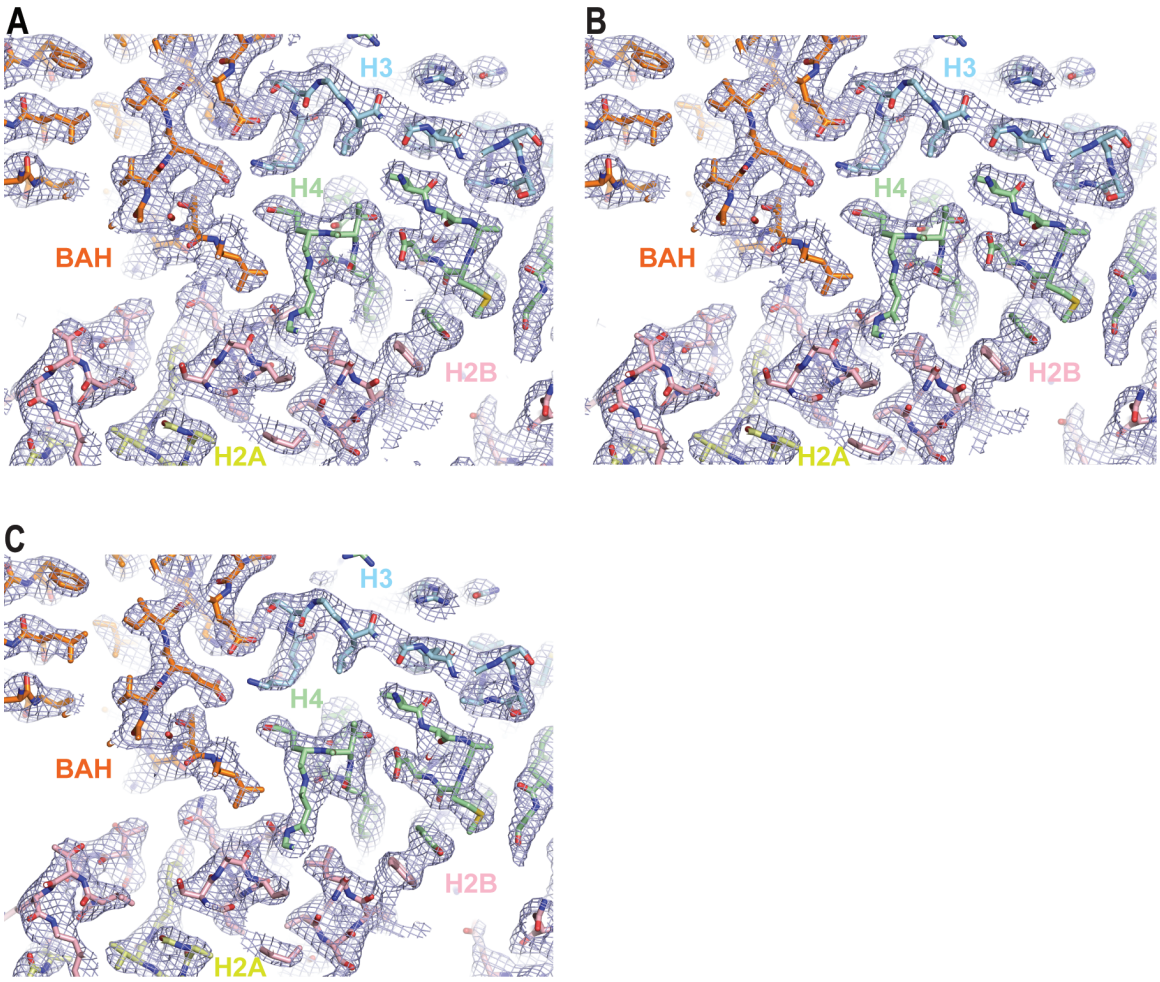

Fig. S2 Electron density maps
Maximum-likelihood $2mF_o$-DF_c difference Fourier electron density map for BAH-nucleosome body interface contoured at 0.8 σ (**A**), 1.0 σ (**B**) and 1.5 σ (**C**)

Fig. S3 Sequence alignment of regions of Xenopus and yeast histone H2A (color coded the same as structure) and BAH loop 1 with shaded residue found in genetic screens.

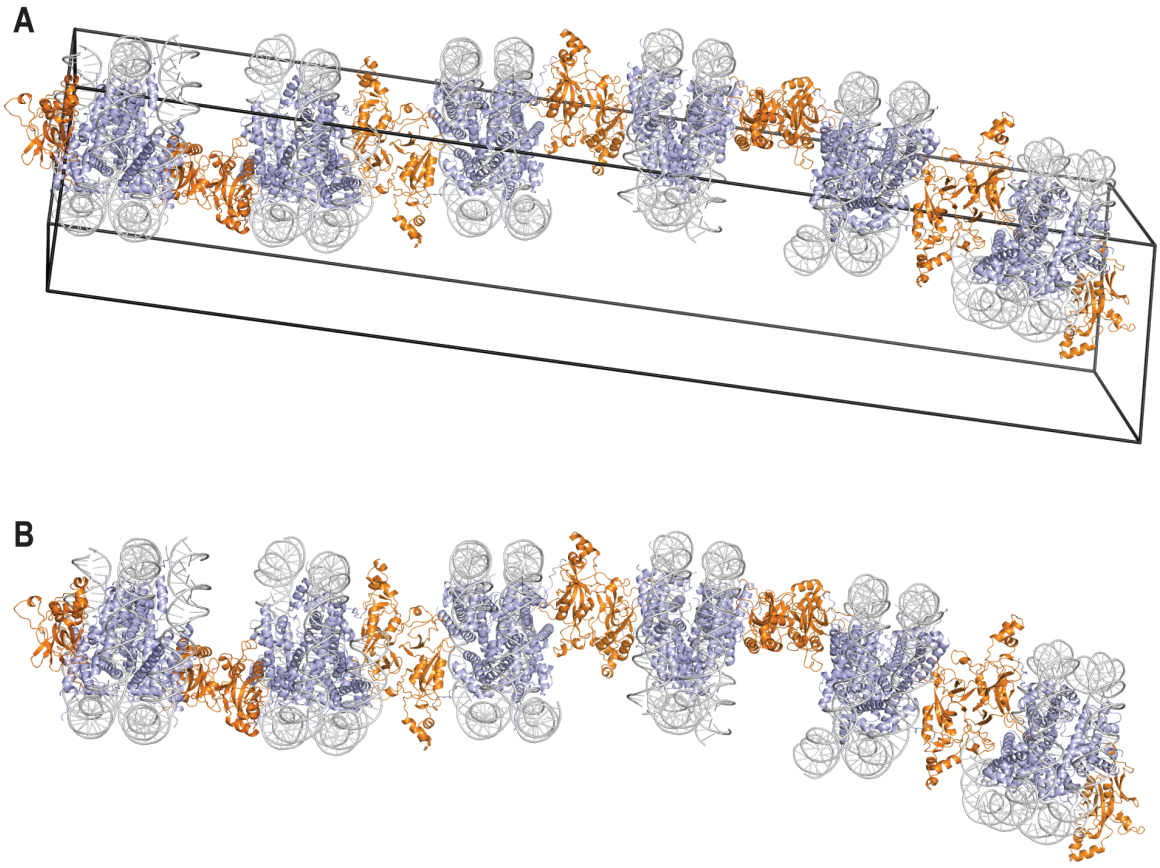

Fig. S4 Crystal packing interaction extended to a unit-cell

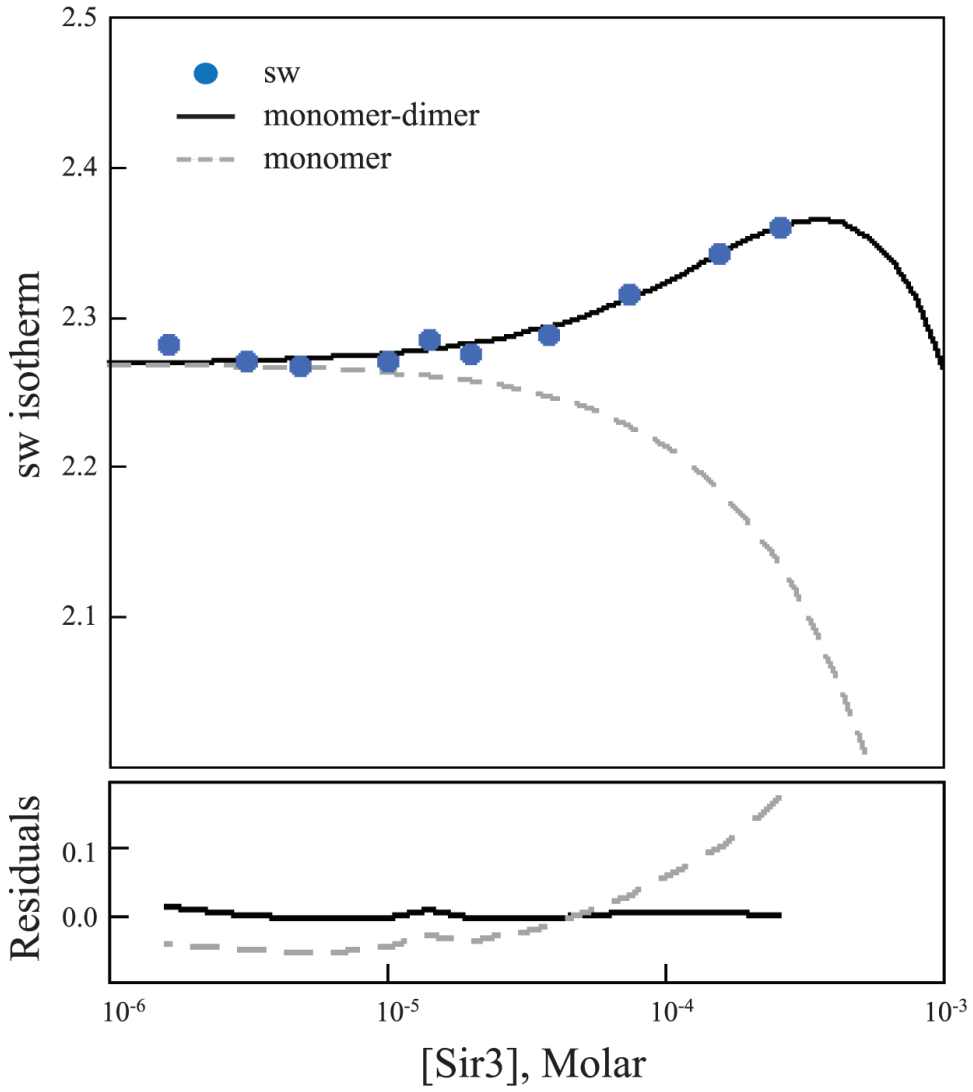

Fig. S5 Isotherm of weight average sedimentation coefficient as a function of total protein concentration. The solid line is a fit to a monomer-dimer model, the dashed line to a monomer only model

Supplementary Table 1

Data collection and refinement statistics

Data Collection

Wavelength	0.97919
Space group	$P6_1$
Cell dimensions	
a, b, c (Å)	102.88 102.88 555.75
α, β, γ (°)	90, 90, 120
Resolution (Å)	50 - 3.0 (3.16 - 3.0)
Mosaicity (°)	0.54
Reflections (total/unique)	368,714/66,264
I/sigmaI	9.1 (2.3)
Completeness (%)	100.0 (100.0)
Redundancy	5.6 (5.6)
R_{merge} (%)	9.9 (68.6)
$R_{r.i.m.}$ (%)	11.0 (75.7)
$R_{p.i.m.}$ (%)	4.7 (31.7)

Refinement

*R*work/*R*free	18.4%/24.1%
Number of atoms	15638
Protein	9652
DNA	5986
Water	0
B-factors (Å^2)	103.8
Protein	82.9
DNA	137.5
R.m.s deviations	
Bond lengths (Å)	0.011
Bond angles (°)	1.591
Ramachandran plot[a]	
Favored (%)	95.7
Allowed (%)	4.1
Outliers (%)	0.2

The highest resolution shell is shown in parentheses. R_{merge} is the merging R factor. $R_{r.i.m.}$ is the redundancy independent merging R factor. $R_{p.i.m.}$ is the precision-indicating merging R factor. For definitions, see Weiss (2001)(*54*)

[a] Calculated using the program Molprobity

References

1. L. N. Rusche, A. L. Kirchmaier, J. Rine, *Annu Rev Biochem* **72**, 481 (2003).
2. S. Loo, J. Rine, *Annu Rev Cell Dev Biol* **11**, 519 (1995).
3. S. J. McBryant, C. Krause, C. L. Woodcock, J. C. Hansen, *Mol Cell Biol* **28**, 3563 (Jun, 2008).
4. F. Martino *et al.*, *Mol Cell* **33**, 323 (Feb 13, 2009).
5. A. Johnson *et al.*, *Mol Cell* **35**, 769 (Sep 24, 2009).
6. P. S. Kayne *et al.*, *Cell* **55**, 27 (Oct 7, 1988).
7. P. C. Megee, B. A. Morgan, B. A. Mittman, M. M. Smith, *Science* **247**, 841 (Feb 16, 1990).
8. E. C. Park, J. W. Szostak, *Mol Cell Biol* **10**, 4932 (Sep, 1990).
9. L. M. Johnson, P. S. Kayne, E. S. Kahn, M. Grunstein, *Proc Natl Acad Sci U S A* **87**, 6286 (Aug, 1990).
10. L. M. Johnson, G. Fisher-Adams, M. Grunstein, *EMBO J* **11**, 2201 (Jun, 1992).
11. J. H. Park, M. S. Cosgrove, E. Youngman, C. Wolberger, J. D. Boeke, *Nat Genet* **32**, 273 (Oct, 2002).
12. J. S. Thompson, M. L. Snow, S. Giles, L. E. McPherson, M. Grunstein, *Genetics* **163**, 447 (Jan, 2003).
13. M. N. Kyriss, Y. Jin, I. J. Gallegos, J. A. Sanford, J. J. Wyrick, *Mol Cell Biol* **30**, 3503 (Jul, 2010).
14. J. Dai, E. M. Hyland, A. Norris, J. D. Boeke, *Genetics* **186**, 813 (Nov, 2010).
15. M. Braunstein, R. E. Sobel, C. D. Allis, B. M. Turner, J. R. Broach, *Mol Cell Biol* **16**, 4349 (Aug, 1996).
16. D. J. Mahoney, J. R. Broach, *Mol Cell Biol* **9**, 4621 (Nov, 1989).
17. S. Loo, J. Rine, *Science* **264**, 1768 (Jun 17, 1994).
18. R. Schnell, J. Rine, *Mol Cell Biol* **6**, 494 (Feb, 1986).
19. L. Sussel, D. Shore, *Proc Natl Acad Sci U S A* **88**, 7749 (Sep 1, 1991).
20. K. A. Nasmyth, *Cell* **30**, 567 (Sep, 1982).
21. D. E. Gottschling, O. M. Aparicio, B. L. Billington, V. A. Zakian, *Cell* **63**, 751 (Nov 16, 1990).
22. S. Ehrentraut *et al.*, *Genes Dev* **25**, 1835 (Sep 1, 2011).
23. V. Sampath *et al.*, *Mol Cell Biol* **29**, 2532 (May, 2009).
24. E. M. Stone, C. Reifsnyder, M. McVey, B. Gazo, L. Pillus, *Genetics* **155**, 509 (Jun, 2000).
25. A. Norris, M. A. Bianchet, J. D. Boeke, *PLoS Genet* **4**, e1000301 (Dec, 2008).
26. J. R. Buchberger *et al.*, *Mol Cell Biol* **28**, 6903 (Nov, 2008).
27. J. J. Connelly *et al.*, *Mol Cell Biol* **26**, 3256 (Apr, 2006).
28. Materials and methods are available as supporting material on *Science* Online.
29. R. D. Makde, J. R. England, H. P. Yennawar, S. Tan, *Nature* **467**, 562 (Sep 30, 2010).
30. F. van Leeuwen, P. R. Gafken, D. E. Gottschling, *Cell* **109**, 745 (Jun 14, 2002).
31. Z. Hou, J. R. Danzer, C. A. Fox, J. L. Keck, *Protein Sci* **15**, 1182 (May, 2006).
32. K. Luger, A. W. Mader, R. K. Richmond, D. F. Sargent, T. J. Richmond, *Nature* **389**, 251 (Sep 18, 1997).

33. Q. Yu, L. Olsen, X. Zhang, J. D. Boeke, X. Bi, *Genetics* **188**, 291 (Jun, 2011).
34. C. J. Fry, A. Norris, M. Cosgrove, J. D. Boeke, C. L. Peterson, *Mol Cell Biol* **26**, 9045 (Dec, 2006).
35. O. M. Aparicio, B. L. Billington, D. E. Gottschling, *Cell* **66**, 1279 (Sep 20, 1991).
36. M. Oppikofer *et al.*, *EMBO J*, (Jun 10, 2011).
37. G. J. Hoppe *et al.*, *Mol Cell Biol* **22**, 4167 (Jun, 2002).
38. K. Luo, M. A. Vega-Palas, M. Grunstein, *Genes Dev* **16**, 1528 (Jun 15, 2002).
39. L. N. Rusche, A. L. Kirchmaier, J. Rine, *Mol Biol Cell* **13**, 2207 (Jul, 2002).
40. J. C. Tanny, D. S. Kirkpatrick, S. A. Gerber, S. P. Gygi, D. Moazed, *Mol Cell Biol* **24**, 6931 (Aug, 2004).
41. M. Onishi, G. G. Liou, J. R. Buchberger, T. Walz, D. Moazed, *Mol Cell* **28**, 1015 (Dec 28, 2007).
42. A. Hecht, T. Laroche, S. Strahl-Bolsinger, S. M. Gasser, M. Grunstein, *Cell* **80**, 583 (Feb 24, 1995).
43. Y. Park, J. Hanish, A. J. Lustig, *Genetics* **150**, 977 (Nov, 1998).
44. C. Liu, A. J. Lustig, *Genetics* **143**, 81 (May, 1996).
45. M. S. Singer *et al.*, *Genetics* **150**, 613 (Oct, 1998).
46. H. H. Ng, D. N. Ciccone, K. B. Morshead, M. A. Oettinger, K. Struhl, *Proc Natl Acad Sci U S A* **100**, 1820 (Feb 18, 2003).
47. A. J. Barbera *et al.*, *Science* **311**, 856 (Feb 10, 2006).
48. H. Liaw, A. J. Lustig, *Mol Cell Biol* **26**, 7616 (Oct, 2006).
49. G. G. Liou, J. C. Tanny, R. G. Kruger, T. Walz, D. Moazed, *Cell* **121**, 515 (May 20, 2005).
50. D. A. King *et al.*, *J Biol Chem* **281**, 20107 (Jul 21, 2006).
51. S. J. McBryant, C. Krause, J. C. Hansen, *Biochemistry* **45**, 15941 (Dec 26, 2006).
52. H. Renauld *et al.*, *Genes Dev* **7**, 1133 (Jul, 1993).
53. A. Hecht, S. Strahl-Bolsinger, M. Grunstein, *Nature* **383**, 92 (Sep 5, 1996).
54. M. Weiss, *Journal of Applied Crystallography* **34**, 130 (2001).
55. J. J. Connelly *et al.*, *Mol Cell Biol* **26**, 3256 (Apr, 2006).
56. K. Luger, T. J. Rechsteiner, T. J. Richmond, *Methods Enzymol* **304**, 3 (1999).
57. A. G. W. Leslie, *Joint CCP4 + ESF-EAMCB Newsletter on Protein Crystallography*, (1992).
58. Collaborative Computational Project Number 4, *Acta Crystallographica Section D* **50**, 760 (1994).
59. A. J. McCoy *et al.*, *Journal of Applied Crystallography* **40**, 658 (2007).
60. C. A. Davey, D. F. Sargent, K. Luger, A. W. Maeder, T. J. Richmond, *J Mol Biol* **319**, 1097 (Jun 21, 2002).
61. E. B. G Bricogne, M Brandl et al.,, *(United Kingdom: Global Phasing Ltd. , Cambridge, 2008)*.
62. P. D. Adams *et al.*, *Acta Crystallographica Section D* **58**, 1948 (2002).
63. P. Emsley, K. Cowtan, *Acta Crystallographica Section D* **60**, 2126 (2004).
64. V. B. Chen *et al.*, *Acta Crystallographica Section D* **66**, 12 (2010).
65. R. A. Laskowski, MacArthur, M. W., Moss, D. S. and Thornton, J. M, *J. Appl. Crystallogr*, 283 (1993).
66. N. A. Baker, D. Sept, S. Joseph, M. J. Holst, J. A. McCammon, *Proc Natl Acad Sci U S A* **98**, 10037 (Aug 28, 2001).

67. W. Kabsch, C. Sander, *Biopolymers* **22**, 2577 (Dec, 1983).
68 A. M. Waterhouse, J. B. Procter, D. M. Martin, M. Clamp, G. J. Barton, *Bioinformatics* **25**, 1189 (May 1, 2009).

This work was supported by grant GM043901 from the NIH (to REK). K-J.A. was supported in part by a fellowship from the Human Frontier Science Program. We thank the staff at Beamlines 24-IDC/E at Argonne National Laboratory, especially K. Rajashankar and F. Murphy for excellent assistance with data collection. We thank T. Schwartz for use of the high-throughput crystallization facility as well as helpful discussions and critical reading of the manuscript. We thank F. Winston and R. Sternglanz for critical reading of the manuscript. We thank S. Jenni and D. Kostrewa for helpful discussions, S.Tan, and K. Luger for help with technical aspects of forming nucleosomes, J.Cochrane, S. Bowman, S. Miller, M. Simon and K. Bouazoune for critical reading of the manuscript, and members of the Kingston laboratory for helpful discussions. Coordinates and structure factors have been deposited in the Protein Data Bank (PDB) with accession code 3TU4.